Asymmetric crystal plasticity theory for the evolution of polycrystal microstructures

P.V. Trusov*, P.S. Volegov, and A.Yu. Yants

Perm State Technical University, Perm, 614990, Russia

Analysis of the lattice geometry and geometric properties of a yield polyhedron in crystal elastoplasticity theory demonstrates the necessity of going to asymmetric measures of stress-strain states in the description of severe plastic deformation of polycrystals with deep micro- and mesostructural rearrangements. A general two-level (macro- and mesolevel) physical theory for describing the evolution of micro- and mesostructures of polycrystals is formulated in which each level is described by strain rate measures and associated stress and strain measures. The elasticity tensor at the mesolevel is analyzed. Separate consideration is given to the choice of macroscale rigid motion. Constitutive relations for the rotational mode are derived, and an algorithm is proposed to determine rotational elements — material regions that experience rotation at a certain point in time. Simulation results for individual particular cases of loading are presented.

Keywords: crystal plasticity theories, asymmetric measures of stress-strain states, asymmetric elasticity, lattice rotation, fragmentation

DOI: 10.1134/S1029959912010067

1. Introduction

The application of the crystal plasticity theories for describing the elastic or inelastic deformation of single- and polycrystalline solids raises an acute question as to what measures of stress-strain states must be chosen. On the one hand, the measures must provide the basis for the derivation of adequate stress-strain relations that describe deformation at a given level; on the other, they must allow for the physical and geometrical peculiarities of the objects for which they are introduced (e.g., asymmetric properties of single crystal lattices (grains, subgrains)). The crystal plasticity theories often use quantities with a vague physical meaning, e.g., so-called orientation tensors of slip systems which appear in an explicit form in constitutive relations, $\mathbf{M}_{\mathrm{S}}^{(k)} = 1/2\,(\mathbf{n}^{(k)}\mathbf{b}^{(k)} + \mathbf{b}^{(k)}\mathbf{n}^{(k)})$. For the given quantity there is a discrepancy between its physical meaning (namely, it characterizes the orientation of the k-th slip system of edge dislocations with the unit vector (directed as the Burgers vector) $\mathbf{b}^{(k)}$ which determines the slip direction, and the slip plane normal $\mathbf{n}^{(k)}$) and the relation that defines the quantity. In this case, e.g., for the face-centered cubic lattice one more slip system with the normal $\mathbf{b}^{(k)}$ and shear direction $\mathbf{n}^{(k)}$ is actually "introduced" into the orientation tensor. If the so-introduced orientation tensor of the (111)[110] slip system is used to describe the irreversible shear kinematics, then owing to symmetrization the orientation tensor equation also "includes" the (110)[111] system, which does not agree with the known crystallographic data. The same holds true for some other tensor quantities used in continuum mechanics and solid mechanics.

In many theories of elastoplastic (and elasto-viscoplastic) crystals the criterion of slip system activation and hence the condition of material transition from the elastic state to plastic flow is the fulfillment of the Schmid law for the given system:

$$\mathbf{b}^{(k)}\mathbf{n}^{(k)} : \mathbf{s} = \tau_{\mathrm{c}}^{(k)}, \tag{1}$$

where k is the number of the slip system, k = 1–24 (for fcc crystals the number of slip systems doubles), and $\mathbf{s}$ is the stress deviator. Generally speaking, the critical shear stress value $\tau_{\mathrm{c}}^{(k)}$ is not constant during deformation and can be different for different slip systems. The set of Schmid's law equations written for all systems determines a hypersurface in the stress space which serves as a boundary between the region of purely elastic deformation and that of elastoplastic deformation, i.e. the yield hypersurface (polyhedron). To construct a physically adequate and mathematically strict

* *Corresponding author*
Prof. Peter V. Trusov, e-mail: tpv@matmod.pstu.ac.ru

theory of plasticity it is necessary first of all to study the yield polyhedron geometry defined by a set of equations of type (1), in order to find the number and order of the polyhedron vertices and edges. The highest possible order of the vertices would demonstrate how much the available approach to the description of deformation on the basis of symmetric measures is mathematically and physically strict and closed. As shown elsewhere [1], if the Schmid law (1) is used as the plasticity criterion, the yield polyhedron for fcc crystals has vertices of the 6-th and 8-th order only (which is also consistent with paper [2]). Thus, when using the symmetric measures of stress-strain states in the crystal elastoplasticity theories a question arises under certain conditions as to what active slip systems must be chosen. Since having only 5 independent stress deviator components and being in a vertex of the sixth or eighth order on the yield surface, it is necessary to determine somehow the 5 systems out of 6 or 8 which will be assumed active in further calculation.

The above reasoning requires such a crystal plasticity theory to be constructed that is free from the physically unjustified symmetrization of the measures of stress-strain states and their rates. The theory must be developed on physically justified assumptions and relations, all quantities used in it must have a clear physical meaning.

The development of such a theory presents some difficulties, as well as those related to an expected increase of the number of constants in constitutive relations, first of all, constitutive equations of elasticity (Hooke's law). A positive point is that the relations of the model are clear. It facilitates the addition to them, if necessary, of additional deformation mechanisms, or the account of different effects arising in severe plastic deformation. These are texturing, fragmentation, hardening and softening, damage accumulation and failure of polycrystals. Besides, the above-mentioned problem of the choice of active slip systems disappears in this case. If an asymmetric strain measure (or asymmetric strain rate measure) is introduced with the incompressibility condition for the irreversible (plastic) component of the measure, we have an 8-dimensional space. This means that, from the viewpoint of the crystal plasticity theories, it becomes possible to choose eight rather than five active slip systems. Even in the "worst" case when the image point of stresses is in the 8-th order vertex the number of equations in the model is sufficient to accurately define shear along all active slip systems.

Attempts to construct mathematical models that describe the meso- and microstructure evolution in a material under various forces and are based on symmetric measures of stress-strain states have been made since 30–50s of the 20th century (G. Taylor [3], J. Bishop, R. Hill [4], T.H. Lin [5] et al.). The Russian scientists have also made a notable advance in describing the processes of severe plastic deformation accompanied by microstructural evolution (O.A. Kaibyshev, R.Z. Valiev [6], Ya.D. Vishnyakov [7], A.N. Orlov [8], V.A. Likhachev [9], V.V. Rybin [10] et al.). Tomsk scientific school (V.E. Panin [11], P.V. Makarov [12] and others) laid the foundation for a new discipline (physical mesomechanics) at the interface of solid mechanics and solid state physics which studies among other things the structural evolution of the material. In the present paper by the crystal plasticity theories are meant a wide class of plasticity theories in which constitutive relations, hypotheses and principles are formulated with an explicit consideration of deformation mechanisms at the meso- and microscale; the development of such theories strongly influenced the studies of the scientists listed.

Most of the modern physical theories that describe the rotation of grains (used, e.g., in the studies on fragmentation and texturing) consider the so-called "material rotation" determined by the orthogonal tensor entering into the polar decomposition of the elastic component of the deformation gradient; in so doing, the elastic distortion of the lattice and the presence of neighboring grains are neglected. Abundant evidence shows, however, that the rotation processes are associated with the shear incompatibility in slip systems of neighboring grains at dislocation glide (V.V. Rybin, I.M. Zhukovskii, N.Yu. Zolotorevskii et al.). In the studies on fragmentation no consideration is usually given to the fact that the characteristic sizes of rotating regions in a crystal vary, even though this effect is well described in physical metallurgy (V.V. Rybin et al.).

Papers [13–15] put forward an approach to the construction of multilevel models (two-level, in the special case) of a polycrystalline aggregate under deformation, and the general structure of constitutive models with internal variables for describing the micro- and mesostructure evolution in the material. In the following, we will also use a two-level model to describe the elastoplastic deformation of a polycrystalline aggregate. For simplicity sake the quantities for the macrolevel are designated by the capital letters, the related parameters for the mesolevel are denoted by the same small letters. The deformation scheme for the macrolevel is specified, for the strain state at the mesolevel (grain, subgrain) we take a modified Voigt hypothesis for the strain rate measure. The Hooke's law in the relaxation form in terms of rate constants is used as a constitutive relation at the macrolevel; the plastic strain rate is determined from the second-level model (mesolevel) by the shear rate in active slip systems, which are in turn determined with a viscous constitutive relation. The deformation processes are assumed to be quasi-static and to occur at low homologous temperatures, which allows neglecting diffusion mechanisms (recrystallization, recovery, formation of impurity atom atmospheres (Cottrell or Suzuki atmospheres)).

2. Asymmetric measures of strain rate and stress

Let us introduce the main kinematic variables necessary for the description of elastoplastic deformation at the

mesolevel (henceforward first-order (simple) materials are considered). A transposed rate gradient is used as the strain rate measure to describe the deformation processes in a continuum:

$$\boldsymbol{\zeta} = \mathbf{v}\hat{\nabla}. \tag{2}$$

At least two configurations must be used, such as reference $\mathbf{K}_0$ and actual $\mathbf{K}_t$. The strain rate tensor $\boldsymbol{\zeta}$ can be represented in the form: $\boldsymbol{\zeta} = \mathbf{v}\hat{\nabla} = \dot{\mathbf{f}} \cdot \mathbf{f}^{-1}$, where $\mathbf{f} = \overset{0}{\nabla}\mathbf{r}^{\mathrm{T}}$ is the transposed deformation gradient at the mesolevel. The site gradient is multiplicatively decomposed into the elastic (reversible) and plastic (irreversible) components: $\mathbf{f} = \mathbf{f}^{\mathrm{e}} \cdot \mathbf{f}^{\mathrm{p}}$. Substituting this relation in the expression for $\boldsymbol{\zeta}$, we have:

$$\begin{aligned}
\boldsymbol{\zeta} &= (\mathbf{f}^{\mathrm{e}} \cdot \mathbf{f}^{\mathrm{p}})^{\bullet} \cdot (\mathbf{f}^{\mathrm{p}})^{-1} \cdot (\mathbf{f}^{\mathrm{e}})^{-1} = \\
&= (\dot{\mathbf{f}}^{\mathrm{e}} \cdot \mathbf{f}^{\mathrm{p}} + \mathbf{f}^{\mathrm{e}} \cdot \dot{\mathbf{f}}^{\mathrm{p}}) \cdot (\mathbf{f}^{\mathrm{p}})^{-1} \cdot (\mathbf{f}^{\mathrm{e}})^{-1} = \\
&= \dot{\mathbf{f}}^{\mathrm{e}} \cdot \mathbf{f}^{\mathrm{p}} \cdot (\mathbf{f}^{\mathrm{p}})^{-1} \cdot (\mathbf{f}^{\mathrm{e}})^{-1} + \mathbf{f}^{\mathrm{e}} \cdot \dot{\mathbf{f}}^{\mathrm{p}} \cdot (\mathbf{f}^{\mathrm{p}})^{-1} \cdot (\mathbf{f}^{\mathrm{e}})^{-1} = \\
&= \dot{\mathbf{f}}^{\mathrm{e}} \cdot (\mathbf{f}^{\mathrm{e}})^{-1} + \mathbf{f}^{\mathrm{e}} \cdot (\dot{\mathbf{f}}^{\mathrm{p}} \cdot (\mathbf{f}^{\mathrm{p}})^{-1}) \cdot (\mathbf{f}^{\mathrm{e}})^{-1}.
\end{aligned} \tag{3}$$

The augend describes reversible (elastic) strains in the continuum, while the addend in such form, generally speaking, cannot be referred to as the plastic strain rate. To represent $\boldsymbol{\zeta}^{\mathrm{p}}$, it is necessary to go to an unloaded configuration $\mathbf{K}^*$ (with the use of the operator $(\mathbf{f}^{\mathrm{e}})^{-1}$), in this configuration $\boldsymbol{\zeta}^{\mathrm{p}*} = \dot{\mathbf{f}}^{\mathrm{p}} \cdot (\mathbf{f}^{\mathrm{p}})^{-1}$ (Fig. 1).

So, to consider the geometrical interpretation of the given transformations, three configurations must be introduced, namely, reference $\mathbf{K}_0$, actual $\mathbf{K}_t$ and unloaded $\mathbf{K}^*$. Figure 1 shows the linear operators that transform an infinitesimal segment dx in the reference configuration into the same segment in the actual and unloaded configuration.

Then, we introduce the strain state measure $\mathbf{q}$ at the mesolevel formally using the definition of the strain rate measure as a derivative of the corresponding (nonholonomic (not expressed through the displacement vector components)) strain measure. In the context of constructing a model suitable for the description of severe plastic deformation in a continuum with regard to rotational modes it is not enough to use a local derivative to determine the strain rate measure by the differentiation of the strain state measure; we must use more adequate approaches to the problem, e.g., co-rotational differentiation:

$$\mathbf{q}^{\mathrm{R}} = \dot{\mathbf{q}} - \boldsymbol{\Omega} \cdot \mathbf{q} + \mathbf{q} \cdot \boldsymbol{\Omega} = \boldsymbol{\zeta} = \mathbf{v}\hat{\nabla}. \tag{4}$$

As a spin at the mesolevel we propose to use the lattice spin $\boldsymbol{\Omega}$, i.e. the tensor associated with the instantaneous rate of lattice rotation. For the macrolevel the choice of quasi-rigid motion requires separate consideration.

3. The choice of quasi-rigid motion at the macrolevel

One of the most frequent questions arising in the development of two-level (and multilevel, in the general case) models is why does redundant information about stresses arises at the macrolevel? Really, on the one hand, stresses at the macrolevel are defined from the Hooke's law (in the relaxation form) in terms of rate constants which involves averaged inelastic strain rates determined in the mesolevel model. On the other hand, the macrostresses can be defined by averaging of the mesostresses. In so doing, it is beyond reason to expect that the stress states calculated by the two methods are identical or at least close.

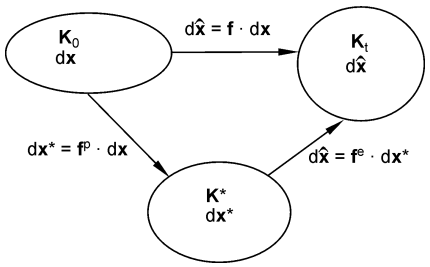

Fig. 1. Schematics of the multiplicative decomposition of the site gradient

It should be remembered, however, that at the macrolevel the problem of the choice of quasi-rigid motion and of a corresponding co-rotational derivative in the Hooke's law remains unsolved. Let $\boldsymbol{\Sigma}$, $\boldsymbol{\sigma}$ respectively stand for the Cauchy stress tensor at the macro- and mesolevel; $\mathbf{Z}$, $\boldsymbol{\zeta}$ are the corresponding strain rate measures; $\mathbf{W}$, $\mathbf{w}$ are the spin tensors for the quasi-rigid motion at the macro- and mesolevel (every time their choice needs consideration depending on the specificity of the problem solved; for example, in our paper $\mathbf{w} = \boldsymbol{\Omega}$), $\mathbf{C}$, $\mathbf{c}$ are the elasticity tensors at the macro- and mesolevel. Use will be made of a modified Voigt hypothesis, $\boldsymbol{\zeta} = \mathbf{Z}$. The averaging operation (not specifying a particular procedure) is denoted by $\langle\ \rangle$. The primed quantities designate the deviation of the fields of the corresponding quantities from the average.

At the macro- and mesolevel the Hooke's law (in the relaxation form) in terms of rate constants is used:

$$\boldsymbol{\Sigma}^{\mathrm{r}} = \mathbf{C} : (\mathbf{Z} - \mathbf{Z}^{\mathrm{p}}), \quad \boldsymbol{\Sigma}^{\mathrm{r}} = \dot{\boldsymbol{\Sigma}} - \mathbf{W} \cdot \boldsymbol{\Sigma} + \boldsymbol{\Sigma} \cdot \mathbf{W}, \tag{5}$$

$$\boldsymbol{\sigma}^{\mathrm{r}} = \mathbf{c} : (\boldsymbol{\zeta} - \boldsymbol{\zeta}^{\mathrm{p}}), \quad \boldsymbol{\sigma}^{\mathrm{r}} = \dot{\boldsymbol{\sigma}} - \mathbf{w} \cdot \boldsymbol{\sigma} + \boldsymbol{\sigma} \cdot \mathbf{w}. \tag{6}$$

Let $\mathbf{C} = \langle \mathbf{c} \rangle$, $\mathbf{c} = \mathbf{C} + \mathbf{c}'$, $\mathbf{Z}^{\mathrm{p}} = \langle \boldsymbol{\zeta}^{\mathrm{p}} \rangle$, $\boldsymbol{\zeta}^{\mathrm{p}} = \mathbf{Z}^{\mathrm{p}} + \boldsymbol{\zeta}^{\mathrm{p}\prime}$, $\mathbf{w} = \langle \mathbf{w} \rangle + \mathbf{w}'$, $\boldsymbol{\Sigma} = \langle \boldsymbol{\sigma} \rangle$, $\boldsymbol{\sigma} = \boldsymbol{\Sigma} + \boldsymbol{\sigma}'$. Rewrite the relation (6) as:

$$\begin{aligned}
&\dot{\boldsymbol{\Sigma}} - \langle \mathbf{w} \rangle \cdot \boldsymbol{\Sigma} + \boldsymbol{\Sigma} \cdot \langle \mathbf{w} \rangle + \dot{\boldsymbol{\sigma}}' - \mathbf{w}' \cdot \boldsymbol{\Sigma} + \boldsymbol{\Sigma} \cdot \mathbf{w}' + \\
&\quad + \boldsymbol{\sigma}' \cdot \langle \mathbf{w} \rangle - \langle \mathbf{w} \rangle \cdot \boldsymbol{\sigma}' - \mathbf{w}' \cdot \boldsymbol{\sigma}' + \boldsymbol{\sigma}' \cdot \mathbf{w}' = \\
&\quad = \mathbf{C} : (\mathbf{Z} - \mathbf{Z}^{\mathrm{p}}) - \mathbf{C} : \boldsymbol{\zeta}^{\mathrm{p}\prime} + \mathbf{c}' : (\mathbf{Z} - \mathbf{Z}^{\mathrm{p}}) - \mathbf{c}' : \boldsymbol{\zeta}^{\mathrm{p}\prime}.
\end{aligned} \tag{7}$$

Before averaging the above relation, we will analyze (7), the right-hand side first. The averaging of the first term gives the term itself, while that of the second and third gives zero tensors. In the last term, generally speaking, the quantities can be both correlated and uncorrelated. At the same time, the elasticity tensor deviation from the average over a representative volume of the macrolevel is a result of different grain orientation (as well as initial), whereas $\boldsymbol{\zeta}^{\mathrm{p}\prime}$ cha-

racterizes the deviation of the instantaneous, here and now, inelastic strain rate tensor from the average which depends in a random manner on many other characteristics (stresses, hardening in slip systems). This allows, in the first approximation, the quantities of the last term in the right-hand side to be assumed uncorrelated, owing to which the term will also be zero in averaging.

Now turn to the analysis of the left-hand side of (7). In averaging the first three terms remain unchanged, the 4–8th terms in averaging give the true zero. To the last terms we can apply a reasoning similar to the above for the last term of the right-hand side, then in averaging these terms will be equal to zero tensors. Hence, relations (5) and (6) agree when the spin tensor at the macrolevel is defined as the average of the spin tensors at the mesolevel: $\mathbf{W} = \langle \mathbf{w} \rangle$.

We may reject the hypothesis that the quantities in the last two terms of the left-hand side of (7) are uncorrelated. Then, for (5) and (6) to agree, we must assume that:

$$\mathbf{W} = \langle \mathbf{w} \rangle + \boldsymbol{\Sigma}^{-1} \cdot \langle \boldsymbol{\sigma}' \cdot \mathbf{w}' \rangle,$$
$$\mathbf{W}^{\mathrm{T}} = \langle \mathbf{w} \rangle^{\mathrm{T}} + \langle \boldsymbol{\sigma}' \cdot \mathbf{w}' \rangle^{\mathrm{T}} \cdot \boldsymbol{\Sigma}^{-\mathrm{T}} = $$
$$= -\langle \mathbf{w} \rangle - \langle \mathbf{w}' \cdot \boldsymbol{\sigma}' \rangle \cdot \boldsymbol{\Sigma}^{-1}.$$

In the last term the symmetry of the Cauchy stress tensor at the macrolevel is taken into account; in the case of the asymmetric tensor the second term has only $\boldsymbol{\Sigma}^{-\mathrm{T}}$.

4. Asymmetric law of elasticity at the mesolevel

There are two different definitions of elasticity, namely, the Cauchy elasticity (which requires that an elastic potential must exist) and the Green elasticity, for which the requirement is introduced [16]. We will follow the second definition. Notice that in the classical linear mechanics the law of elasticity is derived from the series expansion of the free energy in the vicinity of zero elastic strains. With regard to the initial unstressed and unstrained state we finally arrive at the following relation:

$$\boldsymbol{\sigma}_{ij} = \rho \frac{\partial^2 F}{\partial q^{\mathrm{e}}_{\ ij} \partial q^{\mathrm{e}}_{\ kl}} q^{\mathrm{e}}_{\ kl} = c_{ijkl} q^{\mathrm{e}}_{\ kl}, \ \boldsymbol{\sigma} = \mathbf{c} : \mathbf{q}^{\mathrm{e}}, \tag{8}$$

where $\mathbf{c}$ is the fourth-order tensor that describes the elastic properties of the material, ρ is the density, F is the Helmholtz free energy. It is seen from (8) $\mathbf{c}$ is symmetric with respect to pairs of subscripts: $c_{ijkl} = c_{klij}$. However, we cannot assert the symmetry of $\mathbf{c}$ within the pairs of subscripts because the measures of the stress and strain states are asymmetric at the mesolevel.

To determine the number of nonzero independent components of the elasticity tensor, we use the symmetry properties of the physical object to which the developed theory will be applied, namely, the lattice symmetry of a single crystal. Paper [17], following [18], describes a method that allows, in the general case, obtaining restrictions on the form of the elastic moduli (components of the elasticity tensor $\mathbf{c}$) imposed by the lattice symmetry of the material. For this purpose, rotations relative to the crystal symmetry axes are considered and the invariance conditions for the components of the tensor $\mathbf{c}$ in transition from one coordinate system to another are written. As a result, a number of restrictions are obtained which relate the fourth-order tensor components. As shown in [17], the given algorithm together with the condition of symmetry with respect to pairs of subscripts suggests that for a material with cubic lattice symmetry the elasticity tensor $\mathbf{c}$ has only 4 independent components: $c_{1111}, c_{1122}, c_{1212}, c_{1221}$ (in the crystallographic coordinate system).

Then, following from the above, the asymmetric law of elasticity at the mesolevel can be finally written as:

$$\boldsymbol{\sigma} = \mathbf{c} : \mathbf{q}^{\mathrm{e}}, \tag{9}$$

where $\mathbf{c}$ is the fourth-order tensor having 4 independent components, or in the rate form:

$$\boldsymbol{\sigma}^{\mathrm{r}} = \mathbf{c} : \boldsymbol{\zeta}^{\mathrm{e}}, \tag{10}$$

where $\boldsymbol{\sigma}^{\mathrm{r}}$ is the corresponding co-rotational derivative of the mesolevel introduced above which takes into account the rotation of the lattice-related crystallographic coordinate system as a rigid whole. The law of elasticity for the macrolevel reads:

$$\boldsymbol{\Sigma}^{\mathrm{r}} = \mathbf{C} : (\mathbf{Z} - \mathbf{Z}^{\mathrm{p}}),$$
$$\boldsymbol{\Sigma}^{\mathrm{r}} = \dot{\boldsymbol{\Sigma}} - \mathbf{W} \cdot \boldsymbol{\Sigma} + \boldsymbol{\Sigma} \cdot \mathbf{W}, \quad \mathbf{W} = \langle \boldsymbol{\Omega} \rangle. \tag{11}$$

It is worth noting that the conclusion about the symmetry of the stress state measure (particularly, the Cauchy stress tensor) at one or another scale level must be made reasoning from the presence or absence of physical causes at the given level which act as sources of asymmetry. For the mesolevel the stress measure asymmetry is caused by couple stresses (below we discuss how they arise and are taken into account), while for the macrolevel such causes cannot be identified. Hence for the mesolevel we propose to use an asymmetric Cauchy stress tensor as the asymmetric stress state measure. At the macrolevel stresses are assumed to be symmetric, and the averaging of the elasticity tensor and stresses at the macrolevel goes on simultaneously with symmetrization: $\boldsymbol{\Sigma} = \langle \mathrm{sym}(\boldsymbol{\sigma}) \rangle$, $\mathbf{C}_{ijkl} = 1/(4N) \sum_{m=1}^{N} (c^{(m)}_{ijkl} + c^{(m)}_{jikl} + c^{(m)}_{ijlk} + c^{(m)}_{jilk})$, $i, j, k, l = 1, 2, 3$, where m is the number of a mesolevel element (grain, subsgrain), and N is the number of mesolevel elements entering into a macrolevel element.

Within the given approach an additional difficulty arises: in symmetric theories the values of independent elasticity tensor components are measured experimentally for various single crystals; in our case, however, it is problematic to identify the new elastic constants c_{1212}, c_{1221}. To solve this problem, we performed a series of numerical experiments on simple loading in which all independent component values were determined. In [17] a molecular statics simulation is used to qualitatively analyze the elasticity tensor components c_{1212}, c_{1221}, which reveals some divergence (fractions of a percent) between these values. Below (Section 7) we demonstrate that even an insignificant divergence

between the elasticity tensor components influences greatly the elastoplastic behavior of a representative material volume.

5. Description of lattice rotation and grain fragmentation

The mathematical model developed to describe the micro- and mesostructure evolution in a material under severe plastic deformation must be also appropriate for the description of other effects observed in deformed polycrystals, such as texturing that cannot occur without changes in the orientation of individual grains (subgrains, fragments) during continued inelastic deformation. Owing to this, the model must incorporate both quantities that account for the introduction of a new rotational mode, new variables that reflect the lattice rotation kinematics and, what is most important, physically justified dynamic variables that reflect the causes (induced by forces) of the rotation of grains and their fragments.

Now we introduce the major terms describing the polycrystal structure which will be used in the following. By the "grain" is meant the smallest material volume that (at least in the initial moment of deformation) with adequate accuracy can be considered a single crystal. The term "rotational element" is taken to mean any microstructural constituent (grain, subgrain, fragment) or their aggregate capable of rotating as a whole, with the preservation (with adequate accuracy) of regular crystal lattice of the constituents, their mutual position and orientation (Fig. 2). Note that, generally speaking, the size of the rotational element undergoing rotation is not known in advance. Moreover, experiments show that with growing strain intensity the characteristic sizes of rotating structural elements change [10, 19]. To define a rotational element at every moment of deformation, we introduce one more type of structural elements that can form a rotational element at every moment of deformation (according to a below-discussed algorithm). By "grain fragments" are meant microregions of the material misoriented relative to each other at angles of the order of a few minutes or degrees [10]. The introduced term "rotational element" does not substitute the notion of "grain" and "grain fragment", because generally at an arbitrary moment of deformation a fragment or a group of fragments or a grain (or even an ensemble of grains) can act as a rotational element.

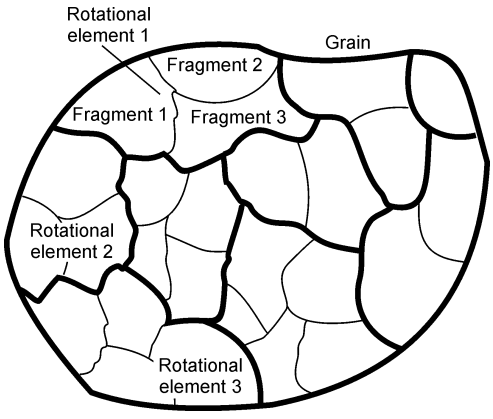

Fig. 2. Structural elements in a polycrystal

In [20] one of the causes of the rotation of the lattice of grains (except for the so-called "material rotation") is considered to be the shear incompatibility in slip systems in neighboring grains (that in turn model the motion of dislocations). Then, the rate of change of the surface couple vector acting on a part of the interface of a considered grain (grain fragment) as a result of resistance to dislocation motion from the given grain (fragment) to neighboring (m = = 1, ..., M) can be defined as a sum:

$$\mathbf{m}^{\mathrm{r}} = \sum_{m=1}^{M} (\mathbf{m}^{\mathrm{r}})^m, \tag{12}$$

where $(\cdot)^r$ is the corresponding co-rotational derivative (the issue of its choice is discussed below), $(\mathbf{m}^{\mathrm{r}})^m$ is the rate component of the couple vector resulting from the incompatibility of shear in the given fragment with shear in the neighboring m-th fragment, and M is the number of neighboring fragments.

The evolution of the couple vector $\mathbf{m}^m$ is defined by the following relation:

$$(\mathbf{m}^{\mathrm{r}})^m = \lambda \mathbf{N} \times \left[\mathbf{L}^{\mathrm{p}\,\mathrm{T}} \right]^m \cdot \mathbf{N}, \tag{13}$$

where λ is an experimentally found (in Pa · m) parameter, $\mathbf{N}$ is the unit normal (external for the studied fragment) to the interface with the neighboring fragment, $\left[\mathbf{L}^{\mathrm{p}\,\mathrm{T}} \right]^m$ is the abrupt change of the plastic component of the rate gradient determined as:

$$\left[\mathbf{L}^{\mathrm{p}\,\mathrm{T}} \right]^m = \sum_{i}^{K} \dot{\gamma}^i \mathbf{n}^i \mathbf{b}^i - \sum_{j}^{K} \dot{\gamma}^{j(m)} \mathbf{n}^{j(m)} \mathbf{b}^{j(m)}, \tag{14}$$

where $\dot{\gamma}^i$, $\dot{\gamma}^{j(m)}$ are the shear rates, $\mathbf{b}^i$, $\mathbf{b}^{j(m)}$ are the unit vectors directed as the Burgers vectors, $\mathbf{n}^i$, $\mathbf{n}^{j(m)}$ are respectively the normals for slip systems in the studied and neighboring fragments, and K is the number of slip systems (24 for an fcc crystal with regard to doubling).

Now define the form of the co-rotational derivative which is necessary to use in relations (12), (13) to observe the principle of material frame indifference. Let a rotational element and all surrounding fragments rotate as a rigid whole. In this case, the couple vector (as well as the couple stress tensor) undergoes the same rotation. Note also that in the calculations for an individual fragment all quantities (strain rate, stresses, elasticity tensor, shear along slip systems, couple forces) are defined from the viewpoint of an observer located in the crystallographic coordinate system; the fragment material is rigidly "fixed" to the same coordinate system. Since the crystallographic coordinate system is rotated relative to the laboratory coordinate system as a

rigid whole (together with the material), then for the principle of material frame indifference to be satisfied it is necessary to choose such a co-rotational derivative that would be "fixed" to the angular rotation rate of the lattice:

$$\mathbf{m}^{\mathrm{r}} = \dot{\mathbf{m}} - \boldsymbol{\Omega}\cdot\mathbf{m} + \mathbf{m}\cdot\boldsymbol{\Omega}, \tag{15}$$

where $\boldsymbol{\Omega}$ is the spin tensor of the fragment lattice determined at every moment of deformation as the tensor associated with the angular rotation rate vector of the lattice $\boldsymbol{\omega}$, $\boldsymbol{\Omega} = -\in\cdot\boldsymbol{\omega}$, with $\in$ being the Levi-Civita tensor.

Hence, for the surface couples we finally have:

$$(\mathbf{m}^{\mathrm{r}})^m = \lambda\mathbf{N}\times\Big(\sum_i^K \dot{\gamma}^i\mathbf{n}^i\mathbf{b}^i - \sum_j^K \dot{\gamma}^{j(m)}\mathbf{n}^{j(m)}\mathbf{b}^{j(m)}\Big)\cdot\mathbf{N}. \tag{16}$$

However, the beginning of rotations is influenced, in the general case, by two components: couple forces (or the associated couple stresses) arising due to the incompatibility of plastic strains in neighboring grains, and (generally speaking) the asymmetric part of the Cauchy stress tensor which also produces a torque of a couple on the rotational element surface. Indeed, let e.g. $\sigma_{12} \neq \sigma_{21}$, then unbalanced shear forces arise on the rotational element surface which produce a torque of a couple. If $\sigma_{12} > \sigma_{21}$, this torque is directed along the unit vector $\mathbf{k}_3$ in the positive direction. Thus, relations for the lattice rotation rates must be derived with consideration for the both force factors: couple stresses and torques due to the asymmetric part of the Cauchy stress tensor.

In order to determine both the rotational element size and the value of the lattice spin of the rotational element, we need to "reduce" all dynamical causes of rotation (surface couples on all parts of the rotational element interface, asymmetric Cauchy stresses) to an equivalent quantity, which we propose to be the body couple:

$$\mathbf{M}^i = \frac{1}{V^i}\sum_{m=1}^{M}\Big[\mathbf{m}^m S_m^i + \mathbf{r}^m\times(\mathbf{N}^m\cdot\boldsymbol{\sigma}^i)S_m^i\Big], \tag{17}$$

where $[\mathbf{M}^i]$ (Pa) is the body couple vector acting on the rotational element i due to the incompatibility of dislocation motion along slip systems of fragments of the given rotational element and the neighboring fragments belonging to other rotational elements, S_m^i is the area of a flat region of the interface m between two rotational elements, V^i is the volume of the given rotational element, $\mathbf{r}^m$ is the radius vector from the center of mass of the rotational element to the midpoint of the facet m, $\boldsymbol{\sigma}^i$ is the Cauchy stress tensor acting in the given region of the rotational element, and $\mathbf{N}^m$ is the external normal to the facet m. The second term of the right-hand side of (17) defines an additional component of the torque arising at the rotational element boundary because of an asymmetric (in the general case) stress state.

In the present paper we put forward the following algorithm of defining the region of rotation and the criterion of grain rotation.

1. Initially, each grain G is a set of fictitious fragments (in contrast to rotational elements which are defined at every moment of deformation by a special algorithm considered below) that have the same orientation as the grain G (Fig. 2).

2. To define the set of fragments that experience plastic rotation as a whole at a given moment of deformation (i.e. to define a rotational element), we propose a "growing pattern" scheme: starting with triple (and more) grain junctions we define the smallest set of fragments g of the grain G such that the body couple calculated for the given set according to formulas (12)–(17) reads:

$$\mathbf{M}^G = \frac{1}{V}\sum_{g=1}^{N^G}\Big[\mathbf{m}^g S_g + \mathbf{r}^g\times(\mathbf{N}^g\cdot\boldsymbol{\sigma}^g)S_g\Big], \tag{18}$$

where the upper summation limit N^G emphasizes that the summation is taken over the outer boundaries for the given set, and reaches a critical value:

$$|\mathbf{M}^G| \geq M_{\mathrm{c}}, \tag{19}$$

which is a material parameter in the general case (or even a material function):

$$M_{\mathrm{c}} = M_{\mathrm{c}}(\Psi, \alpha_1, ..., \alpha_n),$$

where $\Psi = \int_{\tau=0}^{t}\sqrt{\boldsymbol{\Omega}:\boldsymbol{\Omega}}\,\mathrm{d}\tau$ is the accumulated "plastic" rotation of the lattice, and $\alpha_1, ..., \alpha_n$ is the set of internal variables (the shape and size of the given rotational element, the density of orientation misfit dislocations accumulated in the boundaries by the current point in time, etc.). Notice that much experimental evidence counts in favor of taking into account the smallest material volume undergoing plastic rotation. The data show that the rotation of fragments begins with the rotation of small regions adjacent to grain junctions by small misorientation angles [10, 19, et al.]. In further calculations this set of fragments is assumed to be a rotational element at a given moment of deformation, i.e. for all fictitious fragments of the given physical grain fragment the lattice spin at the given moment is the same.

After the rotational elements are defined, we must calculate the rotation rate of the crystallographic coordinate system for the given rotational element; in so doing, it is important that the tensor defining the lattice rotation has an orthogonality property. Therefore, the rotation at each integration step is described with the use of the orthogonal tensor $\Delta\mathbf{R} = (\cos\Delta\varphi + 1)\mathbf{e}\mathbf{e} + \cos\Delta\varphi\mathbf{I} + \sin\Delta\varphi\mathbf{e}\times\mathbf{I}$ ($\mathbf{I}$ is the second-order unit tensor) which determines the coordinate system rotation about the instantaneous rotation axis $\mathbf{e}$ by an angle $\Delta\varphi$, with the direction of $\mathbf{e}$ being assumed coaxial with the body couple vector

$$\mathbf{e}^G = \frac{\mathbf{M}^G}{|\mathbf{M}^G|}$$

and for the angular rotation rate we take the hypothesis of additivity and single-curve hypothesis:

$$\dot{\varphi}^G = \begin{cases} \dfrac{1}{A}|\dot{\mathbf{M}}^G| + \dfrac{1}{H}|\mathbf{M}^G| \\ \text{if } |\mathbf{M}^G| = M_c \text{ and } \mathbf{M}^G \cdot \dot{\mathbf{M}}^G > 0, \\ \dfrac{1}{A}\left|\dot{\mathbf{M}}^G\right| \\ \text{if } |\mathbf{M}^G| \neq M_c \text{ and } \mathbf{M}^G \cdot \dot{\mathbf{M}}^G \leq 0, \end{cases} \quad (20)$$

where A, H are the experimentally determined material parameters.

Generally speaking, the critical value of the couple force M_c must be determined each time for the given rotational element, because the rotational element surface at a given moment of deformation can present a set of grain boundary regions, low-angle boundaries arising due to small rotations of neighboring rotational elements at previous points in time as well as "internal" boundaries (i.e. fictitious boundaries of fragments within the grain which have not yet rotated); in this case, the pattern of critical stress variation in different fragments is different. The critical couple forces must also depend on the shape of the rotational element: the more spherical it is, the smaller must be the forces needed for the lattice to rotate. Hence, the critical M_c value in the first approximation is calculated as follows:

$$M_c = \frac{1}{V}\sum_{g=1}^{N^G}\left[|\mathbf{r}^g \times (\tau_c^g \mathbf{N}^g)|\, S_g\right], \quad (21)$$

where M_c (Pa) is the critical value of the body couple, S_g is the area of the facet of the boundary fragment g entering into the considered rotational element, τ_c^g (Pa) is the average critical stress for slip systems of the boundary element, N^G is the number of boundary fragments of the given rotational element, and V is the rotational element volume; the summation is taken over the "boundary" fragments of the rotational element. Broadly speaking, for each boundary region of the rotational element it is necessary to formulate evolutionary equations for the critical stresses, in the first approximation they are assumed to be average for the slip systems of the fragment.

6. Structure of the asymmetric theory for the mesolevel

Below we enumerate the major hypotheses of the mesolevel model:

1. The strain rate measure **z** can be represented as a sum of two components: reversible strain rate $\boldsymbol{\zeta}^e$ and irreversible strain rate $\boldsymbol{\zeta}^p$:

$$\boldsymbol{\zeta} = \mathbf{v}\hat{\nabla} = \boldsymbol{\zeta}^e + \boldsymbol{\zeta}^p, \quad (22)$$

where $\boldsymbol{\zeta}^e = \dot{\mathbf{f}}^e \cdot (\mathbf{f}^e)^{-1}$ and $\boldsymbol{\zeta}^p = \mathbf{f}^e \cdot (\dot{\mathbf{f}}^p \cdot (\mathbf{f}^p)^{-1}) \cdot (\mathbf{f}^e)^{-1}$.

2. The total strain rates of individual grains $\boldsymbol{\zeta}_{(n)}$ are equal to the total strain rate of a polycrystalline aggregate (a Voigt hypothesis analog is taken):

$$\boldsymbol{\zeta}_{(n)} = \boldsymbol{\zeta} = \mathbf{Z}, \ \forall n. \quad (23)$$

However, it does not follow from the equality of the strain rate measures in grains that the strain measures are equal, because at each moment of deformation the grains can have different angular rotation rates (owing to the introduction of co-rotational derivatives for defining the stress-strain state measure).

3. The incompressibility condition may be imposed on the irreversible strain rate (because as the irreversible deformation mechanisms we will consider the motion of dislocations, twinning and slipping of crystal parts relative to each other, which preserve their volume):

$$\begin{aligned} I_1(\boldsymbol{\zeta}^p) &= I_1(\mathbf{f}^e \cdot (\dot{\mathbf{f}}^p \cdot (\mathbf{f}^p)^{-1}) \cdot (\mathbf{f}^e)^{-1}) = \\ &= \mathrm{sp}(\mathbf{f}^e \cdot (\dot{\mathbf{f}}^p \cdot (\mathbf{f}^p)^{-1}) \cdot (\mathbf{f}^e)^{-1}) = \\ &= \mathrm{sp}((\mathbf{f}^e)^{-1} \cdot \mathbf{f}^e \cdot (\dot{\mathbf{f}}^p \cdot (\mathbf{f}^p)^{-1})) = \\ &= \mathrm{sp}(\dot{\mathbf{f}}^p \cdot (\mathbf{f}^p)^{-1}) = I_1(\dot{\mathbf{f}}^p \cdot (\mathbf{f}^p)^{-1}) = 0. \end{aligned} \quad (24)$$

4. The irreversible deformation occurs through shear along particular crystallographic systems, shearing along slip systems is described with the viscoplastic law of the form

$$\dot{\gamma}^{(k)} = \dot{\gamma}_0 H(\tau^{(k)} - \tau_c^{(k)}) \left|\frac{\tau^{(k)}}{\tau_c^{(k)}}\right|^{1/m} \mathrm{sign}\,\tau^{(k)}, \quad (25)$$

where m is the strain-rate sensitivity parameter of the material [21], $\dot{\gamma}_0$ is the characteristic shear rate, $\tau^{(k)} = \mathbf{b}_k \mathbf{n}_k : \mathbf{s}$ is the effective shear stress in the k-th slip system, $\tau_c^{(k)}$ is the critical shear stress value in the given slip system governed by the hardening law, H is the Heaviside function, and **s** is the stress deviator.

At any moment of deformation (through dislocation glide) the irreversible strain rate is expressed as:

$$\boldsymbol{\zeta}^p = \mathbf{f}^e \cdot \left(\sum_{k=1}^{K} \mathbf{b}^{(k)} \mathbf{n}^{(k)} \dot{\gamma}^{(k)}\right) \cdot (\mathbf{f}^e)^{-1}, \quad (26)$$

where K is the number of active slip systems.

The rate of change of the critical shear stresses in each slip system is defined by a function of the total shear along slip systems as well as of the shear rates (by the hardening law

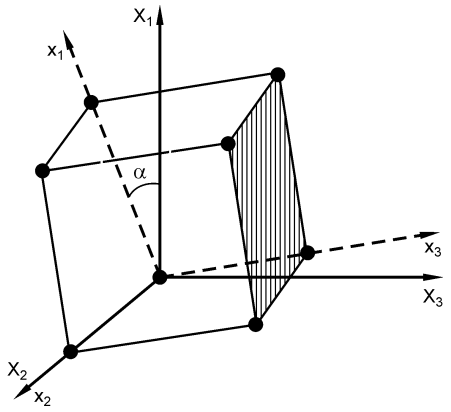

Fig. 3. Relative position of the axes of the laboratory and crystallographic coordinate systems

[14, 22]):

$$\dot{\tau}_c^{(k)} = f(\gamma^{(i)}, \dot{\gamma}^{(j)}), i, j = \overline{1,24}. \quad (27)$$

Using the above-introduced rate form of the Hooke's law it is easy to derive an expression for the stress rate:

$$\boldsymbol{\sigma}^{\mathrm{r}} = \mathbf{c} : \left(\mathbf{v}\hat{\nabla} - \mathbf{f}^{\mathrm{e}} \cdot \left(\sum_{k=1}^{K} \mathbf{b}^{(k)} \mathbf{n}^{(k)} \dot{\gamma}^{(k)} \right) \cdot (\mathbf{f}^{\mathrm{e}})^{-1} \right). \quad (28)$$

Before describing the numerical results obtained with the constructed mathematical model, we will formulate the complete statement of the mesolevel problem to verify the mathematical completeness:

$$\begin{cases} \dot{\gamma}^k = \dot{\gamma}_0 H(\mathbf{n}_i \mathbf{b}_i : \mathbf{s} - \tau_{\mathrm{c}}^k) \left| \dfrac{\mathbf{n}_i \mathbf{b}_i : \mathbf{s}}{\tau_{\mathrm{c}}^{(k)}} \right|^{1/m} \operatorname{sign} \tau^k, \\ \mathbf{s} = \operatorname{dev} \boldsymbol{\sigma}, \; k = \overline{1,24}, \\ \dot{\tau}_{\mathrm{c}}^{(k)} = f(\gamma^{(i)}, \dot{\gamma}^{(j)}), i, j = \overline{1,24}, \\ \dot{\mathbf{f}}^{\mathrm{p}} \cdot (\mathbf{f}^{\mathrm{p}})^{-1} = \mathbf{f}^{\mathrm{e}} \cdot \left(\sum_{i=1}^{24} \dot{\gamma}_i \mathbf{b}_i \mathbf{n}_i \right) \cdot (\mathbf{f}^{\mathrm{e}})^{-1}, \\ \dot{\boldsymbol{\sigma}} = \mathbf{c} : \left(\boldsymbol{\zeta} - \mathbf{f}^{\mathrm{e}} \cdot \left(\sum_{k=1}^{K} \mathbf{b}_k \mathbf{n}_k \dot{\gamma}^k \right) \cdot (\mathbf{f}^{\mathrm{e}})^{-1} \right) - \\ \quad - \boldsymbol{\sigma} \cdot \boldsymbol{\Omega} + \boldsymbol{\Omega} \cdot \boldsymbol{\sigma}, \\ \boldsymbol{\zeta}_{(n)} = \boldsymbol{\zeta}, \\ \text{the algorithm for defining rotational elements,} \\ \mathbf{M} = \dfrac{1}{V} \sum_{m=1}^{M} \left[\left\{ \lambda \, \mathbf{N}^m \times \left(\sum_{i=1}^{24} \dot{\gamma}_i \mathbf{n}_i \mathbf{b}_i - \sum_{j=1}^{24} \dot{\gamma}_{j(m)} \mathbf{n}_{j(m)} \mathbf{b}_{j(m)} \right) \cdot \mathbf{N}^m + \right. \right. \\ \quad \left. \left. + \boldsymbol{\Omega} \cdot \mathbf{m}_i - \mathbf{m}_i \cdot \boldsymbol{\Omega} \right\} S_m^i + \mathbf{r}^m \times (\mathbf{N}^m \cdot \boldsymbol{\sigma}) S_m^i \right], \\ \mathbf{e} = \dfrac{\mathbf{M}}{|\mathbf{M}|}, \; \boldsymbol{\Omega} = \dot{\mathbf{R}} \cdot \mathbf{R}^{\mathrm{T}}, \\ \dot{\varphi} = \begin{cases} \dfrac{1}{A} |\dot{\mathbf{M}}| + \dfrac{1}{H} |\mathbf{M}|, |\mathbf{M}| = M_{\mathrm{c}} \text{ and } \mathbf{M} \cdot \dot{\mathbf{M}} > 0, \\ \dfrac{1}{A} |\dot{\mathbf{M}}|, |\mathbf{M}| \neq M_{\mathrm{c}} \text{ and } \mathbf{M} \cdot \dot{\mathbf{M}} \leq 0, \end{cases} \\ M_{\mathrm{c}} = \dfrac{1}{V} \sum_{g=1}^{N^G} \left[\left| \mathbf{r}^g \times (\tau_{\mathrm{c}}^g \mathbf{N}^g) \right| S_g \right], \\ \Delta \mathbf{R} = (\cos \Delta\varphi + 1) \mathbf{e}\mathbf{e} + \cos \Delta\varphi \mathbf{I} + \sin \Delta\varphi \mathbf{e} \times \mathbf{I}. \end{cases} \quad (29)$$

The analysis of the system of equations (29) suggests that the statement of the problem is correct: at each moment of deformation we have 49 scalar and 5 tensor equations of the second order to determine 49 scalar and 5 tensor unknowns of the second order for each rotational element.

7. Numerical results

First we will give some results obtained in the study on how the elasticity tensor asymmetry influences the elastoplastic behavior of the material. We performed a number of numerical experiments on uniaxial compression of a single crystal that was differently oriented with respect to the loading axis. To purposefully analyze the influence of the asymmetry of the measures, hardening in slip systems was neglected in the experiments. All stress-strain state problems (for the meso- and macrolevel) are solved incrementally, an explicit Euler integration scheme is used. Compression was performed along the X_1 axis of the laboratory coordinate system, the lattice orientation was defined by the angle between the x_1 and X_1 axes in the crystallographic and laboratory coordinate systems, respectively, at the alignment of the x_2 and X_2 axes (Fig. 3). Despite uniaxial compression the crystal was deformed in all possible slip systems.

Figure 4 shows the stress-strain curves for the single crystal in the context of the symmetric (Fig. 4(*a*)) and asym-

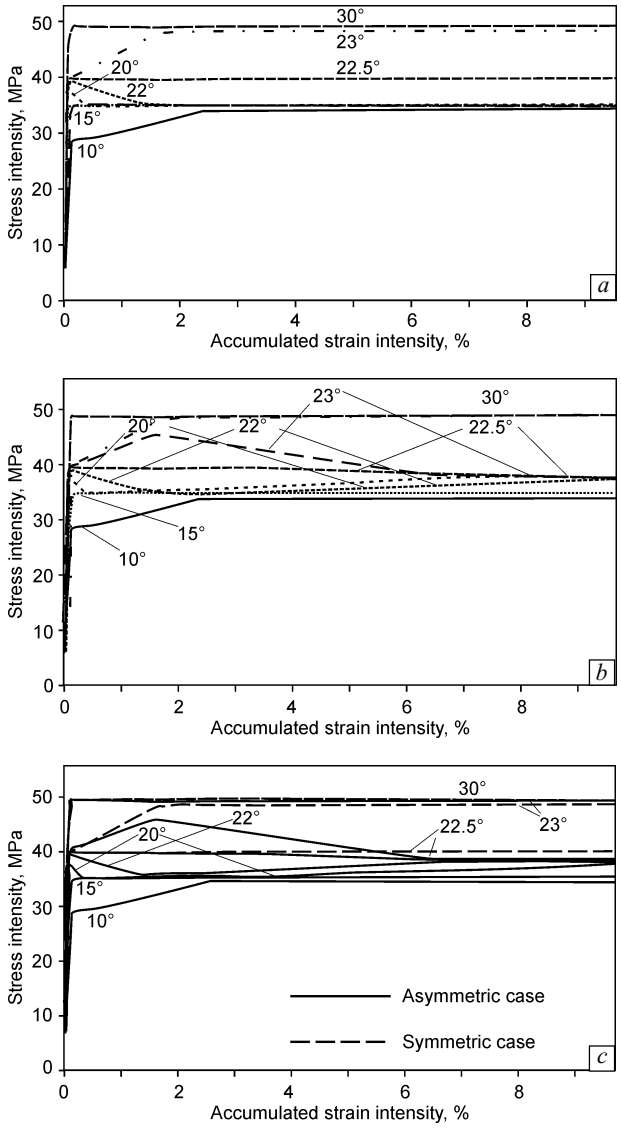

Fig. 4. Stress intensity versus accumulated strain intensity $q_{\mathrm{i}} = \sqrt{2/3 \mathbf{q} : \mathbf{q}}$ under uniaxial compression of a single crystal, at different orientations: symmetric physical theory being used (*a*); asymmetric measures being used (*b*); comparison of the curves for some orientations (*c*)

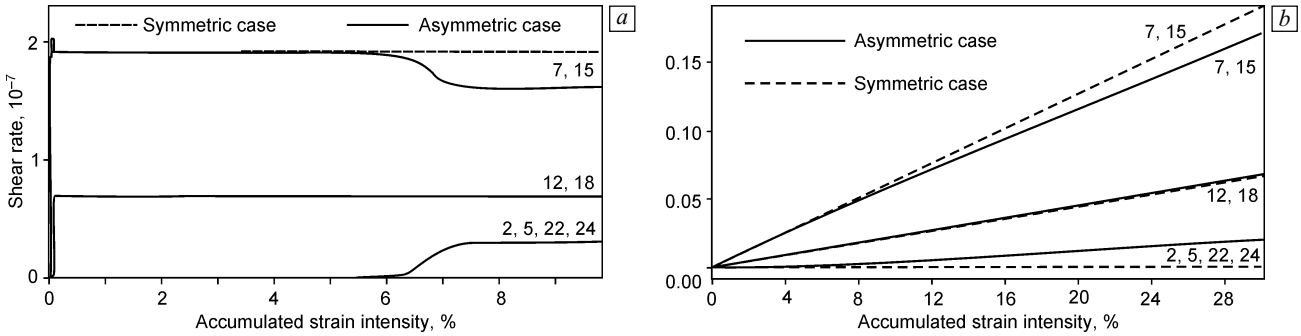

Fig. 5. Shear rate (*a*) and accumulated shear (*b*) for active slip systems versus accumulated strain intensity at 22.5° orientation, comparison of the symmetric and asymmetric theories, slip systems are numerated according to Table 1

metric (Fig. 4(*b*)) crystal elastoplasticity theories at different orientations of the crystallographic coordinate system of the single crystal relative to the laboratory coordinate system. The asymmetric elasticity tensor components c_{1212}, c_{1221} are assumed to differ from the corresponding modulus c_{1212} for the symmetric measures as 0.995 and 1.005 respectively (the material is copper). Noticeable is the presence of two attractor-curves corresponding to orientations of 15° and 30° which the diagram tends to depending on the orientation angle as well as the presence of the instability region in the diagram at an orientation of 22.5°.

There are some characteristic features of the diagrams plotted for the symmetric and asymmetric case (at the same values of the elastic moduli):

– for the majority of orientations, the curve corresponding to the asymmetric case lies below the curve corresponding to the symmetric theory (Fig. 4(*c*));

– the least deviation of the two diagrams is in the region of 0° and 45° orientations, the largest occurs at a 22.5° misorientation angle of the laboratory and crystallographic coordinate systems.

We have plotted the dependence of the shear rate in active slip systems on the accumulated strain intensity for the case of the symmetric and asymmetric theories for 22.5° orientation, the results are given in Fig. 5(*a*). In the asymmetric theory at 6 % strain intensity there occurs shear redistribution over 8 slip systems, while in the symmetric theory the number of active slip systems is invariant and equal to 4. Figure 5(*b*) demonstrates the dependences of the accumulated shear along slip systems on the accumulated strain intensity at 22.5° orientation for the symmetric and asymmetric theories. The behavior of the curves is seen to be different: in some systems slipping is more intensive in the case of the asymmetric theory, in others vice versa; nevertheless, the total shear along all slip systems at the given orientation is somewhat larger in the asymmetric theory.

Now consider some results concerning the deformation of a polycrystal consisting of a set of differently oriented grains with regard to lattice rotations; the fragmentation of individual grains is not considered in the present paper. At the macrolevel the scheme of deformation is defined, at the mesolevel the modified Voigt hypothesis is taken (see Sec-

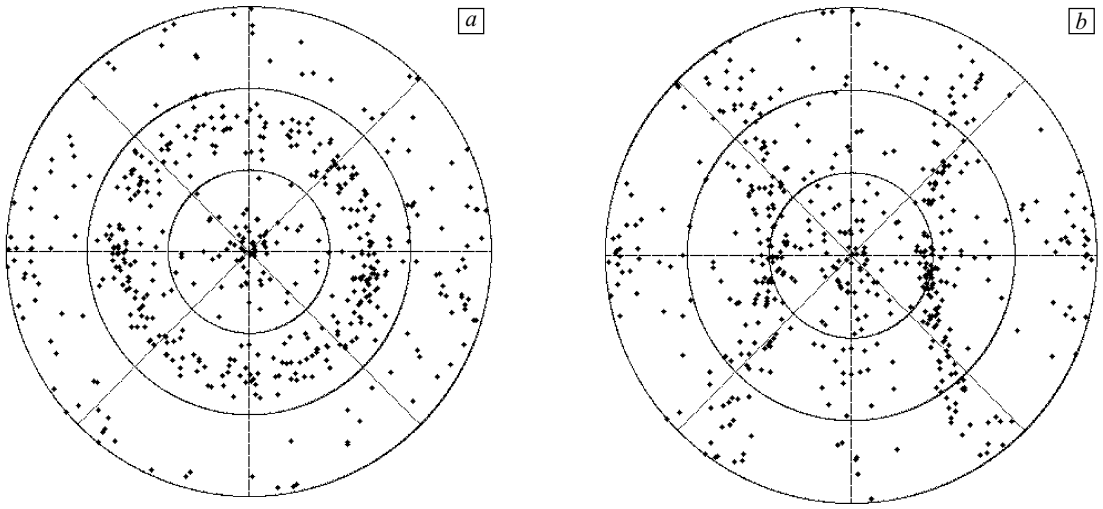

Fig. 6. Stereographic projections of [100] lattice directions of grains after specimen deformation: projection along the OX_1 (*a*) and OX_3 (*b*) axes

Table 1

Burgers vectors and slip system normals

Slip system No.	Burgers vector **b**	Normal vector **n**	Slip system No.	Burgers vector **b**	Normal vector **n**
1	$\frac{1}{\sqrt{2}};0;-\frac{1}{\sqrt{2}}$	$\frac{1}{\sqrt{3}};\frac{1}{\sqrt{3}};\frac{1}{\sqrt{3}}$	13	$-\frac{1}{\sqrt{2}};0;\frac{1}{\sqrt{2}}$	$\frac{1}{\sqrt{3}};\frac{1}{\sqrt{3}};\frac{1}{\sqrt{3}}$
2	$0;\frac{1}{\sqrt{2}};-\frac{1}{\sqrt{2}}$	$\frac{1}{\sqrt{3}};\frac{1}{\sqrt{3}};\frac{1}{\sqrt{3}}$	14	$0;-\frac{1}{\sqrt{2}};\frac{1}{\sqrt{2}}$	$\frac{1}{\sqrt{3}};\frac{1}{\sqrt{3}};\frac{1}{\sqrt{3}}$
3	$\frac{1}{\sqrt{2}};-\frac{1}{\sqrt{2}};0$	$\frac{1}{\sqrt{3}};\frac{1}{\sqrt{3}};\frac{1}{\sqrt{3}}$	15	$-\frac{1}{\sqrt{2}};\frac{1}{\sqrt{2}}0;$	$\frac{1}{\sqrt{3}};\frac{1}{\sqrt{3}};\frac{1}{\sqrt{3}}$
4	$\frac{1}{\sqrt{2}};\frac{1}{\sqrt{2}};0$	$-\frac{1}{\sqrt{3}};\frac{1}{\sqrt{3}};\frac{1}{\sqrt{3}}$	16	$-\frac{1}{\sqrt{2}};-\frac{1}{\sqrt{2}};0$	$-\frac{1}{\sqrt{3}};\frac{1}{\sqrt{3}};\frac{1}{\sqrt{3}}$
5	$\frac{1}{\sqrt{2}};0;\frac{1}{\sqrt{2}}$	$-\frac{1}{\sqrt{3}};\frac{1}{\sqrt{3}};\frac{1}{\sqrt{3}}$	17	$-\frac{1}{\sqrt{2}};0;-\frac{1}{\sqrt{2}}$	$-\frac{1}{\sqrt{3}};\frac{1}{\sqrt{3}};\frac{1}{\sqrt{3}}$
6	$0;\frac{1}{\sqrt{2}};-\frac{1}{\sqrt{2}}$	$-\frac{1}{\sqrt{3}};\frac{1}{\sqrt{3}};\frac{1}{\sqrt{3}}$	18	$0;-\frac{1}{\sqrt{2}};\frac{1}{\sqrt{2}}$	$-\frac{1}{\sqrt{3}};\frac{1}{\sqrt{3}};\frac{1}{\sqrt{3}}$
7	$\frac{1}{\sqrt{2}};\frac{1}{\sqrt{2}};0$	$\frac{1}{\sqrt{3}};-\frac{1}{\sqrt{3}};\frac{1}{\sqrt{3}}$	19	$-\frac{1}{\sqrt{2}};-\frac{1}{\sqrt{2}};0$	$\frac{1}{\sqrt{3}};-\frac{1}{\sqrt{3}};\frac{1}{\sqrt{3}}$
8	$0;\frac{1}{\sqrt{2}};\frac{1}{\sqrt{2}}$	$\frac{1}{\sqrt{3}};-\frac{1}{\sqrt{3}};\frac{1}{\sqrt{3}}$	20	$0;-\frac{1}{\sqrt{2}};-\frac{1}{\sqrt{2}}$	$\frac{1}{\sqrt{3}};-\frac{1}{\sqrt{3}};\frac{1}{\sqrt{3}}$
9	$0;\frac{1}{\sqrt{2}};-\frac{1}{\sqrt{2}}$	$\frac{1}{\sqrt{3}};-\frac{1}{\sqrt{3}};\frac{1}{\sqrt{3}}$	21	$-\frac{1}{\sqrt{2}};0;\frac{1}{\sqrt{2}}$	$\frac{1}{\sqrt{3}};-\frac{1}{\sqrt{3}};\frac{1}{\sqrt{3}}$
10	$\frac{1}{\sqrt{2}};0;\frac{1}{\sqrt{2}}$	$\frac{1}{\sqrt{3}};\frac{1}{\sqrt{3}};-\frac{1}{\sqrt{3}}$	22	$-\frac{1}{\sqrt{2}};0;-\frac{1}{\sqrt{2}}$	$\frac{1}{\sqrt{3}};\frac{1}{\sqrt{3}};-\frac{1}{\sqrt{3}}$
11	$\frac{1}{\sqrt{2}};-\frac{1}{\sqrt{2}};0$	$\frac{1}{\sqrt{3}};\frac{1}{\sqrt{3}};-\frac{1}{\sqrt{3}}$	23	$-\frac{1}{\sqrt{2}};\frac{1}{\sqrt{2}};0$	$\frac{1}{\sqrt{3}};\frac{1}{\sqrt{3}};-\frac{1}{\sqrt{3}}$
12	$0;\frac{1}{\sqrt{2}};\frac{1}{\sqrt{2}}$	$\frac{1}{\sqrt{3}};\frac{1}{\sqrt{3}};-\frac{1}{\sqrt{3}}$	24	$0;-\frac{1}{\sqrt{2}};-\frac{1}{\sqrt{2}}$	$\frac{1}{\sqrt{3}};\frac{1}{\sqrt{3}};-\frac{1}{\sqrt{3}}$

tion 6), the stress state in each grain is determined according to the system of equations (29). The macrostresses are calculated by averaging of the mesostresses with simultaneous symmetrization (see Section 4 for details).

We studied a specimen consisting of 512 grains subjected to uniaxial compression along the OX_1 axis (up to strain intensity 0.6), the initial lattice orientations were set by a random uniform law. Although the macrospecimen is loaded uniaxially, the mesoelements undergo three-dimensional deformation. Figure 6 illustrates the final stereographic projections of [100] grain directions, and figure 7 shows the trajectories of arbitrarily chosen points, which was initially uniformly distributed on the projection plane, during deformation. The analysis of the final positions of the stereographic projections points to a consistency of the rotations. The study of the trajectories of the stereographic

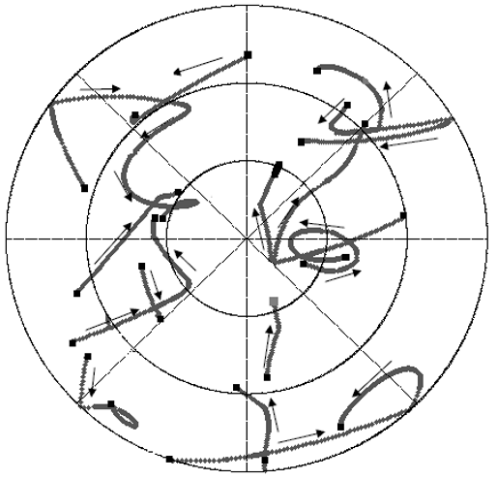

Fig. 7. Stereographic projections of the trajectories of [100] lattice directions of grains during deformation, projection along the OX_1 axis

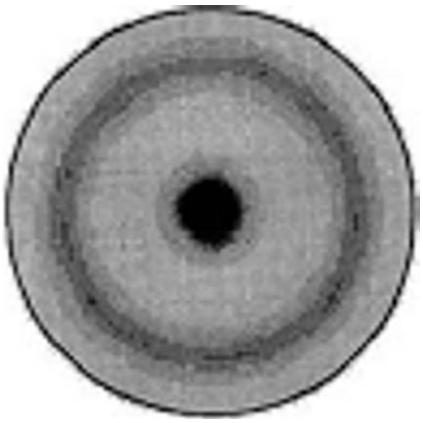

Fig. 8. Experimental data for compression along the OX_1 axis [24]: pole figures for [100] directions, projection along the OX_1 axis

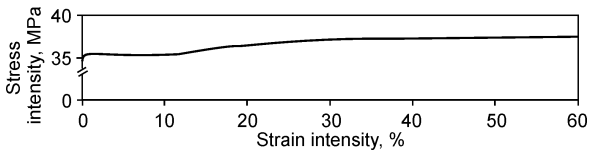

Fig. 9. Stress-strain diagram for the uniaxial compression of a grain aggregate with regard to rotations

projections of individual points suggests that a major part of grains rotates about trajectories which are close to the ones experimentally known for the so-called axial texture (a stationary circular trajectory, or the grains nearly stop) [23, 24] (Fig. 8).

Besides, in the same numerical experiment we plotted a stress-strain curve for an aggregate of 512 grains without hardening in slip systems (Fig. 9). As is seen, at the most intensive rotations (accumulated macrostrain intensity from 12 to 25 %) stresses in the diagram slightly increase. This is most likely related to the process when the system "excitates", during which one can see a stage-like (relay-race) character of the lattice rotations and, consequently, a growing inhomogeneity in the distribution of the rotations. After the phase of active rotations ends and an ordered distribution of the grain orientations is established the system again reaches dynamic equilibrium, which is expressed at the macrolevel as a return to perfect plasticity.

8. Conclusions

The paper considers the issues concerning the construction of the polycrystal plasticity theory, which takes into account the grain lattice rotations, on the basis of asymmetric measures of stress-strain states. A two-level model of elasto-viscoplastic deformation of a polycrystalline aggregate is put forward, the issue of the choice of quasi-rigid motion at the macrolevel is studied. The performed numerical experiments on the uniaxial compression of a polycrystal are in a good agreement with the experimental data.

The work has been financially supported by RFBR (Grants Nos. 10-08-96010-r_Ural_a and 10-08-00156-a).

References

[1] P.S. Volegov, A.S. Nikityuk, and A.Yu. Yants, Yield surface geometry and hardening laws in physical theories of plasticity, Vestnik PGTU: Mathematical Modeling of Systems and Processes, Izd-vo PGTU, Perm, No. 17 (2009) 25 (*in Russian*).

[2] D. Kuhlmann-Wilsdorf, J.T. Moore, E.A. Starke, and S.S. Kulkarni, Deformation bands, the LEDS theory, and their importance in texture development: Part I. Previous evidence and new observations, Metall. Mater. Trans. A., 30, No. 9 (1999) 2491.

[3] G.I. Taylor, Plastic strain in metals, J. Inst. Metals, 62 (1938) 307.

[4] J. Bishop and R. Hill, A theoretical derivation of the plastic properties of a polycrystalline center-faced metal, Philos. Mag., 42 (1951) 414.

[5] T.H. Lin, Physical theory of plasticity, in *Advances in Applied Mechanics*, 11 (1971) 255.

[6] O.A. Kaibyshev and R.Z. Valiev, Grain Boundaries and Properties of Metals, Metallurgiya, Moscow, 1987 (*in Russian*).

[7] Ya.D. Vishnyakov, A.A. Babareko, S.A. Vladimirov, and I.V. Egiz, Theory of Texture Formation in Metals and Alloys, Nauka, Moscow, 1979 (*in Russian*).

[8] A.N. Orlov, Grain Boundaries in Metals, Metallurgia, Moscow, 1980 (*in Russian*).

[9] V.A. Likhachev and V.G. Malinin, Structure-Analytical Theory of Strength, Nauka, Saint Petersburg, 1993 (*in Russian*).

[10] V.V. Rybin, High Plastic Strains and Fracture of Metals, Metallurgia, Moscow, 1986 (*in Russian*).

[11] V.E. Panin, The physical foundations of the mesomechanics of a medium with structure, Russ. Phys. J., 35, No. 4 (1992) 305.

[12] P.V. Makarov, Modeling of deformation and fracture at the mesolevel, Izv. AN, Mekh. Tv. Tela, No. 5 (1999) 109 (*in Russian*).

[13] P.V. Trusov, V.N. Ashikhmin, P.S. Volegov, and A.I. Shveykin, Constitutive relations and their application to the description of microstructure evolution, Phys. Mesomech., 13, No. 1–2 (2010) 38.

[14] P.V. Trusov and P.S. Volegov, Internal variable constitutive relations and their application to description of hardening in single crystals, Phys. Mesomech., 13, No. 3–4 (2010) 152.

[15] P.V. Trusov, V.N. Ashikhmin, and P.S. Volegov, Two-Level Model of Single Crystal Plastic Deformation, in *Mathematical Models and Methods of Continuum Mechanics*, IAPU DVO RAN, Vladivostok (2007) 259 (*in Russian*).

[16] A.I. Lurie, Nonlinear Theory of Elasticity, North-Holland, Amsterdam, 1990.

[17] P.S. Volegov and A.V. Shulepov, Elastic constants of a single crystal in the asymmetric physical theory of plasticity, Vestnik PGTU: Mechanics, No. 1 (2010) 19 (*in Russian*).

[18] K.F. Chernykh, An Introduction to Modern Anisotropic Elasticity, Begell Publishing House, New York, 1998.

[19] S.Yu. Mironov, V.N. Danilenko, M.M. Myshlyaev, and A.V. Korneva, Analysis of the spatial orientation distribution of building blocks in polycrystals as determined using transmission electron microscopy and a backscattered electron beam in a scanning electron microscope, Phys. Solid State, 47, No. 7 (2005) 1258.

[20] P.V. Trussov, V.N. Ashikhmin, and A.I. Shveykin, Two-level model for polycrystalline materials elastoplastic deformation, J. Compos. Mech. Design, 15, No. 3 (2009) 327 (*in Russian*).

[21] S. Balasubramanian and L. Anand, Elasto-viscoplastic constitutive equations for polycrystalline fcc materials at low homologous temperatures, J. Mech. Phys. Solids, 50, No. 1 (2002) 101.

[22] P.V. Trusov, P.S. Volegov, and A.Yu. Yants, Description of intragranular and grain-boundary hardening of single- and polycrystals, Scientific and Technical Bulletin of StPSTU: Physical and Mathematical Sciences, 98, No. 2 (2010) 110 (*in Russian*).

[23] G. Wassermann and J. Grewen, Texturen Metallischer Werkstafte, Springer Verlag, Berlin, 1962.

[24] L. Anand, Single-crystal elasto-viscoplasticity: Application to texture evolution in polycrystalline metals at large strains, Comput. Meth. Appl. Mech. Eng., 193, No. 48–51 (2004) 5359.